nzsee
NEW ZEALAND SOCIETY FOR EARTHQUAKE ENGINEERING

Assessment of boundary conditions for 2D geotechnical site-response analysis with soil heterogeneity

C.A. de la Torre, B.A. Bradley & C.R. McGann
University of Canterbury, New Zealand.

ABSTRACT

This paper examines various boundary condition assumptions for modelling 2D geotechnical site response, which requires a more sophisticated treatment of the boundary and loading conditions than what is typically required in conventional 1D site-response analysis. This study investigates several of the boundary conditions that are typically used for 2D finite element analyses, and assesses their influence on and appropriateness for modelling 2D site response of heterogeneous soil deposits. It is part of a wider study that incorporates soil heterogeneity to model wave scattering and the spatial variability of ground motion in site-response analysis, however, this paper focuses on the boundary conditions and modelling configuration used in the analyses. Several lessons learned and recommendations for conducting such analyses in OpenSees are shared. The results reveal that in order to prevent spurious reflections from the base, a vertically and horizontally compliant base should be used, and each node along the base must be allowed to respond independently with its own dashpot (i.e., base nodes should not be tied to each other to respond in unison). Failure to implement such compliance and independence in the base nodes could result in overestimation of intensity measures (i.e., inefficient absorption of energy) because of the generation of vertical motion from refraction and wave scattering, and the lateral variation in arrival times of down-going waves at the base.

1 INTRODUCTION

In conventional 1D site-response analyses, soil layers are modelled as homogenous, horizontal, and laterally infinite. These assumptions neglect important 2D/3D ground motion phenomena that ultimately influence the response at the ground surface. In order to extend site-response models to 2D, various assumptions and modifications to the boundary conditions must be made. The standard boundary conditions for 1D site-response analysis using the finite element method with a purely horizontal input are periodic lateral boundary conditions (i.e., a node on the left boundary is tied to the corresponding node at the same elevation on the right boundary) and a base that is fixed in the vertical (Y) direction. Not all finite element codes have these boundary

conditions included by default, therefore, the analyst may be required to implement them. For this reason, when 2D problems are analysed, these simplifications that apply to 1D problems are often adopted.

The use of boundary condition simplifications, such as those appropriate for 1D analyses, can cause unintended consequences when used in 2D problems. de la Torre et al. (2021) developed an approach for modelling wave scattering and the spatial variability of ground motion in 2D geotechnical site-response analysis by modelling soil heterogeneity through correlated random fields. They performed a sensitivity study involving 5,400 2D model realisations to investigate the influence of random field input parameters on wave scattering and site response. They found that using standard boundary conditions from 1D site response for 2D site response with soil heterogeneity resulted in strange behaviour observed in transfer functions at the fundamental frequency of the soil deposit. In an attempt to resolve this, an extensive examination of the boundary conditions was launched to determine if they were the cause of this behaviour.

The results of this boundary conditions assessment is included in this current paper. Five different model configurations are compared by making incremental modifications to the boundary conditions. This includes two variations on lateral boundary conditions (periodic versus massive free field columns) and four variations on base conditions (nodes fixed in the vertical direction, and tied to move horizontally uniformly). The most influential modification was releasing the base nodes so that they can each act independently in the horizontal direction and are not all tied to displace uniformly. First, a description of the model geometry, modelling assumptions and boundary conditions used in final production models is provided in Section 2. Next, in Section 3, the various incremental modifications to boundary conditions that led to the final configuration are explained and the influence of each is shown visually.

2 SITE RESPONSE FINAL MODEL CONFIGURATION

For the purpose of the initial sensitivity study by de la Torre et al. (2021), a simple model with a single viscoelastic soil layer over bedrock was considered. This simplification was adopted so that the theoretical behaviour of modelling a heterogeneous soil deposit with spatially correlated random fields was well understood before proceeding to more complex stratigraphy and constitutive response in future work. For all results shown in this paper, the upper layer has a median shear wave velocity ($V_{S,0}$) of 150 m/s, and a compliant base with $V_{S,halfspace}$ = 760 m/s is used to model a soft rock elastic halfspace. Spatial variability in local V_S values is applied to the upper soil layer using a geo-statistical model to create soil heterogeneities that are representative of those observed in geologic deposits.

Figure 1 schematically illustrates many of the features of the site-response model including boundary conditions, location of surface recorder nodes, and an example of a 2D velocity model with anisotropic spatially correlated V_S perturbations. The boundary conditions shown in Figure 1 and described in this section correspond to those of final production models and were selected based on the rigorous examination of different boundary conditions presented in the current work (for lateral boundaries and the base of the model). In Section 3, each component of the boundary conditions and the variations that were examined are described incrementally.

The soil layer above the halfspace is 50 m thick, and the total model width is 1,000 m (1,000 1-m-wide elements). To minimize the influence of lateral boundaries, results are only extracted at 10 equally-spaced nodes within the centre 30% of the model domain, and a 100 m-wide zone of homogeneous soil is included at both lateral extents of the model (i.e., the zero-variance zone). To enforce the free-field 1D deterministic ($1D_{Det}$) response on the lateral boundaries of the model in the production analyses, a massive free-field column is included on each side. The columns are 10 elements (10 m) wide and 10,000 elements thick in the out-of-plain direction. Each column is supported using periodic boundaries on the lateral extents of each column. As shown in Figure 1, the base is fully complaint in the horizontal and vertical directions by connecting each base

node to two dashpots. Additionally, each base node has the appropriate vertical reaction force applied to it so that the model is freely suspended. This vertical compliance is required to prevent spurious reflection of vertical motion generated by wave scattering.

2D viscoelastic site response can be performed in a number of wave propagation codes. OpenSees (McKenna, 2011) was chosen in this study so that complex nonlinear constitutive models can be used in future applications with ease. For computational efficiency, single-integration-point, 4-noded quadratic SSPquad elements (McGann et al., 2012) were used. Elements are sized in the vertical direction such that there are 8 nodes per wavelength at f = 25 Hz (based on the median V_S), however, a maximum element height of 1 m was prescribed so to ensure sufficient discretisation for the heterogeneities.

With the large number of models generated for the de la Torre et al. (2021) sensitivity study, parallelisation of OpenSees and high-performance computing resources were instrumental in executing the analyses. To reduce computation time, each model realisation was parallelised over 8 CPUs using OpenSeesSP. The initial goal was to perform the analyses in 3D, however, the presently poor scalability of OpenSees made it unfeasible to run so many models in 3D (de la Torre et al., 2019). Nonetheless, the sentiments offered in this paper are equally applicable to 3D implementations.

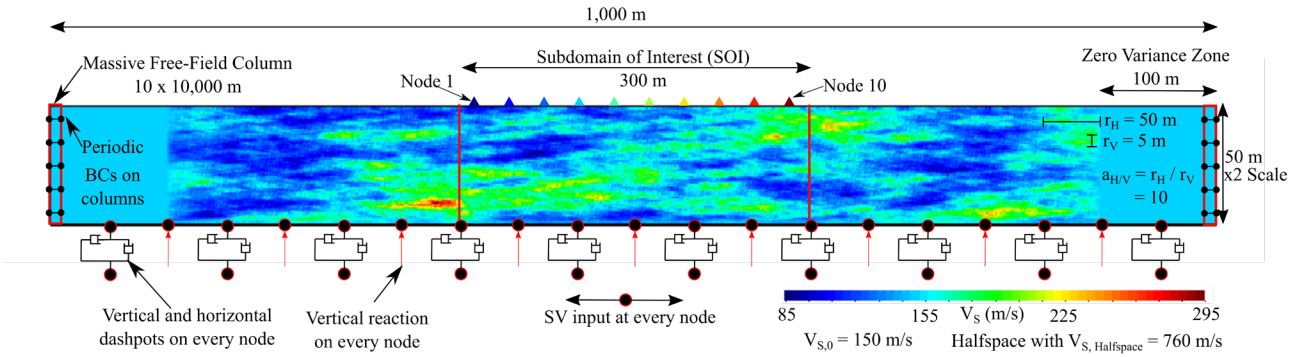

Figure 1: Schematic of site-response model used in de la Torre et al. (2021) production analyses illustrating a 2D shear wave velocity model with heterogeneity, boundary conditions, surface recorder node locations, and zero variance zones. The random field input parameters used for this example are: $V_{S,0}$ = 150 m/s, σ_{lnVs} = 0.175, r_H = 50 m and $a_{H/V}$ = 10. As illustrated, r_H and $a_{H/V}$ are the horizontal correlation length and anisotropy factor, respectively, for random field generation. Note that the vertical scale is stretched by a factor of 2.

3 INCREMENTAL MODIFICATIONS TO BOUNDARY CONDITIONS

As mentioned in the introduction, it is convenient to adopt certain simplifications to boundary conditions for 2D geotechnical analyses, especially when using finite element codes such as OpenSees which do not have these boundary conditions included by default and the analyst is required to implement them. In particular, it is common for 2D dynamic models in OpenSees to be used with periodic boundary conditions ('tiedBoundaries'), a base that is fixed in the vertical direction ('fixedY'), and a base with nodes that are tied in the horizontal (X) direction (i.e., the entire base moves in unison; 'tiedX'). This was the 'control' case that was initially used for this study. Examples of previous studies that have adopted one or all of these boundary condition simplifications are Zhang et al. (2003), Karimi and Dashti (2016), Jeong and Bradley (2017), Gobbi et al. (2017), and Ramirez et al. (2018).

Using this 'control' case with standard boundary conditions from 1D site response for 2D site response with soil heterogeneity resulted in strange behaviour observed in the frequency domain at the fundamental frequency of the soil deposit (f_0). Transfer functions appeared to be distorted (compared to 1D analyses) and showed significantly higher peak amplification at f_0 [AF(f_0)]. This behaviour can be observed directly in nodal and realisation median transfer functions of Figures 2, 3, and 4. To test whether this response was artificially

introduced by the model configuration, a thorough study was launched to identify the cause of this behaviour. Initially, simple things were tested such as: increasing the width of the model (up to 3,000 elements), developing the zero-variance zones, introducing high viscous damping on boundary elements, increasing the duration of the analysis, changing the fundamental frequency of the Ricker wavelet, increasing the total depth of the model, increasing the minimum damping ratio, and modifying how Fourier spectra were computed (e.g, adding more padding and not applying a smoothing function). None of these solutions solved the problem, they all still displayed this odd behaviour in the transfer function, therefore, more significant changes to the boundary conditions were investigated.

The following subsections describe the various components of the boundary conditions, how they were modified, and what influence each assumption has on the response at the ground surface. A direct comparison between methods is made by running the different model configurations with the same 2D randomised V_S models (i.e., the same random seeds) such that the resulting differences in ground response are only attributed to the boundary conditions and not the wave speed of the heterogeneous material. The results from 2D analyses are compared to those from conventional laterally homogeneous 1D site response analyses ($1D_{Det}$) and 1D analyses with randomised profiles extracted as vertical 'slices' from 2D models ($1D_{Rand}$).

3.1 Periodic lateral boundary conditions

The first significant modification to the model configuration was to change the lateral periodic boundary conditions. Rather than tying the lateral boundaries to each other ('tiedBoundaries'), a free field column was approximated on each side by including a massive column (the mass of each element was assigned a mass 10,000 times greater than a standard element by defining the thickness into the page as 10,000 m). These massive columns are within the zero-variance zone, therefore, they have a 1D deterministic velocity profile. The columns enforce this homogeneous "free-field" response on the main model by being significantly more massive than the elements within the main domain. This 2D configuration was verified using a homogeneous velocity model to ensure the response was identical to the control case with periodic boundary conditions. McGann and Arduino (2015), Chin et al. (2016), and de la Maza et al. (2017) are examples of studies that have implemented these massive free field columns in OpenSees. Unlike true free-field boundaries, these massive columns do not absorb all the energy that reaches them from the interior of the model.

Figures 2 and 3 compare results between the two lateral boundary conditions for 2D analyses with velocity perturbations. Figure 2 plots nodal transfer functions ($TF_{i,j}$) for one random field seed while Figure 3 directly compares the resulting realisation median transfer functions ($\overline{TF_j}$) from two random field seeds. While there are slight differences between the two lateral boundary conditions (i.e, the control with periodic boundaries versus the massive free field columns), the response is similar and the strange behaviour around f_0 is still visible. Constraints on the base nodes were analysed next.

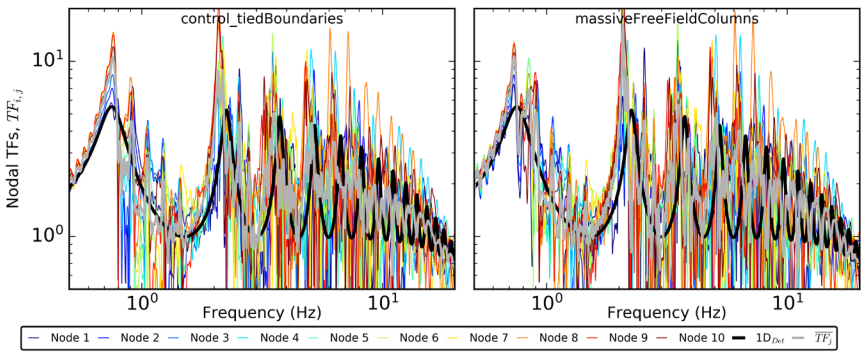

Figure 2: Comparison of nodal transfer functions, $TF_{i,j}$, for two lateral boundary conditions: the control case ('control_tiedBoundaries') and the proposed modification ('massiveFreeFieldColumns').

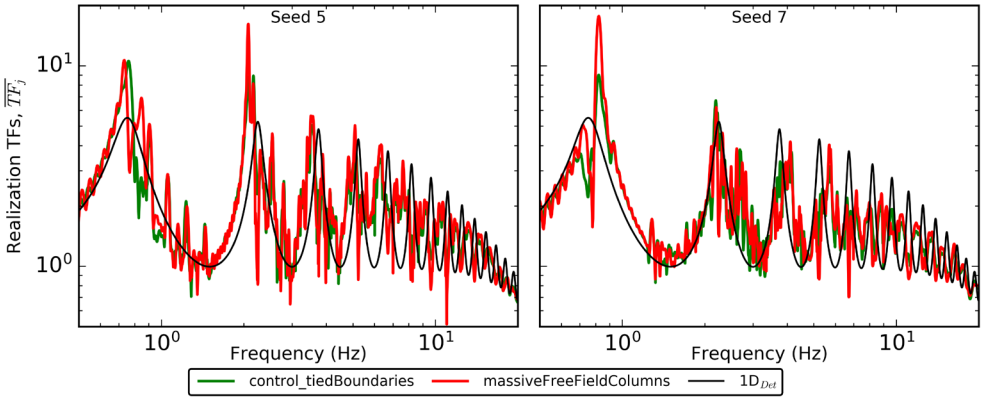

Figure 3: Comparison of realisation mean transfer functions, $\overline{TF_j}$, from two random field seeds for two lateral boundary conditions: the control case ('control_tiedBoundaries') and the proposed modification ('massiveFreeFieldColumns').

3.2 Vertical fixity of base nodes

It is convenient to fix base nodes in the vertical Y direction ('fixedY'), and this idealisation is reasonable when only horizontal motion is present in the model. However, the presence of soil heterogeneity generates surface waves with vertical motion. In order to create a base that is compliant in the vertical direction, to prevent all vertical motion from being trapped in the model, the base nodes cannot be fixed in Y. This also allows for a vertical input motion which was not considered in this study. Releasing the fixity of base nodes ('freeY') requires a multi-step approach in OpenSees. First, the nodes must be fixed in Y and a gravity analysis must be performed to compute the vertical reactions on base nodes. Then the nodes are released, and a force equal to that of the vertical reaction is applied at each node and another gravity analysis is performed for the model to reach equilibrium. Next, dashpots are created at every base node by adding two nodes at the location of each base node. One of these two additional nodes is fully fixed and one is fully free. These dashpot nodes are connected using a zeroLengthElement with a linear viscous material and a dashpot coefficient equal to $\rho V_P A_{trib}$, where ρ = mass density, V_P = compression wave velocity, and A_{trib} = tributary area of column base (i.e., generally 1-element wide). The free dashpot node is then tied to the corresponding main model node using the equalDOF command. Finally, the dynamic analysis can be performed. Note that in OpenSeesSP, when a model is parallelised, incorrect reactions may be recorded at nodes on the boundary of parallel partitions. This is because the nodes exist in two partitions and the reactions are stored as the correct value in one, and as zero on the other. Therefore, the first gravity analysis to record reactions should be performed on a single processor. The heterogeneity in soil stiffness creates non-uniform reactions along the base, therefore, the gravity analysis to record reactions must be performed for every random field realisation.

Figures 4 and 5 plot nodal and realisation transfer functions, respectively, for four model base node conditions. Figure 6 plots other normalized [by 1D deterministic ($1D_{Det}$)] nodal IMs as a function of node position. Comparing the 'fixedY_tiedX' and 'freeY_tiedX' cases allows for assessment of the influence of vertical fixity of base nodes on the response. Releasing the vertical fixities of base nodes has a negligible effect on horizontal IMs, such as transfer functions, the fundamental frequency f_0 and amplification at f_0 ($AF(f_0)$), peak ground acceleration (PGA), spectral acceleration at $1/f_0$ ($SA(T_0)$), and Arias intensity ($I_{a,Hor}$). This is not unexpected as these measures are controlled by the horizontal component of motion. Changes are only visible in vertical IMs such as Arias intensity of the vertical component of accelerations ($I_{a,Vert}$; bottom panels of Fig 6) which shows a notable decrease when the base is free. This effect would be even more pronounced with profiles that have a smaller impedance contrast at the base (currently 150 m/s over 760 m/s). This highlights the significance of considering a vertically compliant base when a 2D profile is not horizontally homogeneous and generates vertical motion.

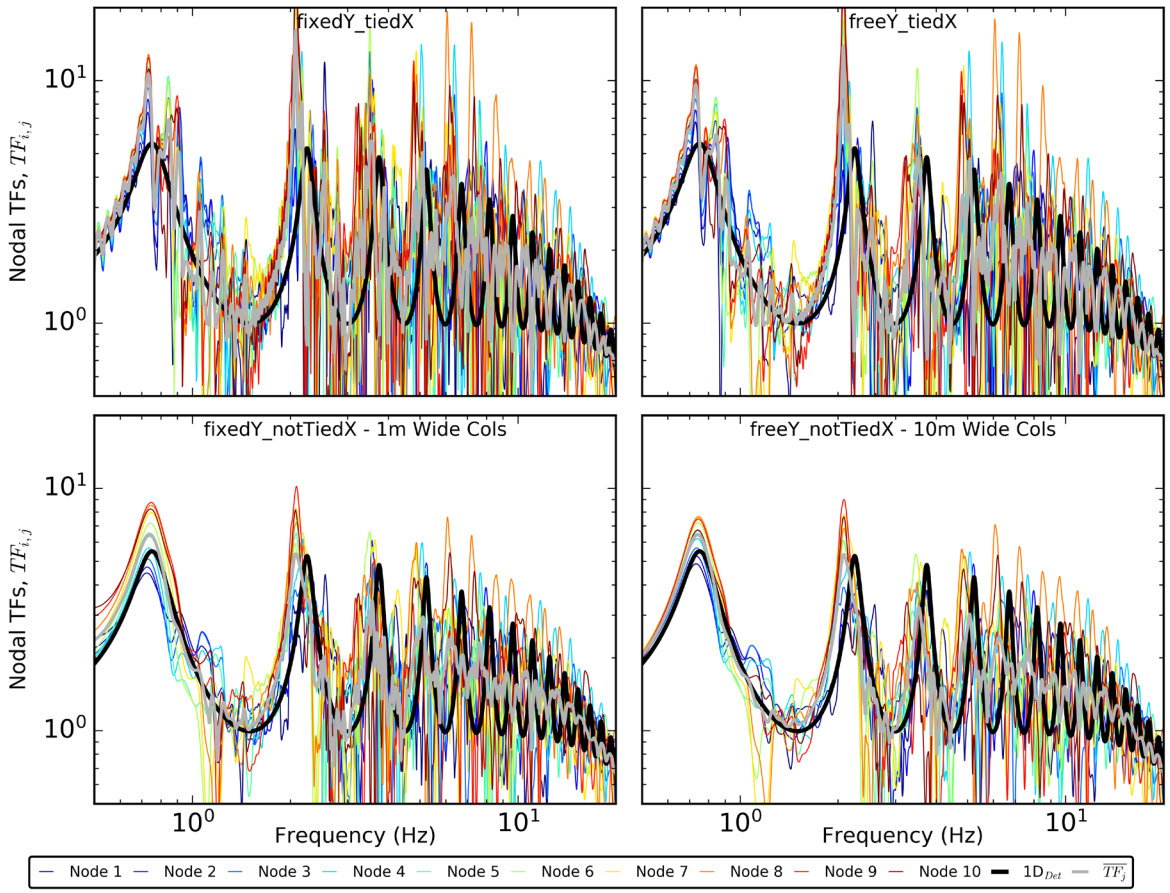

Figure 4: Comparison of nodal transfer functions, $TF_{i,j}$, from one random field seed for four base conditions with massive lateral free field columns for lateral boundaries.

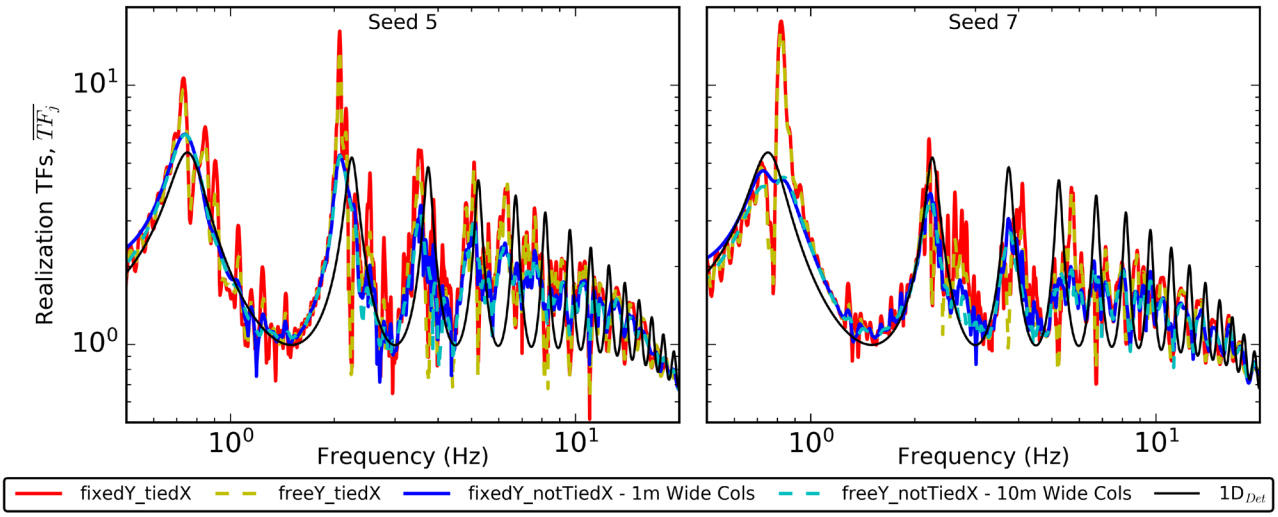

Figure 5: Comparison of realisation median transfer functions, $\overline{TF_j}$, from two random field seeds for four variations on base conditions.

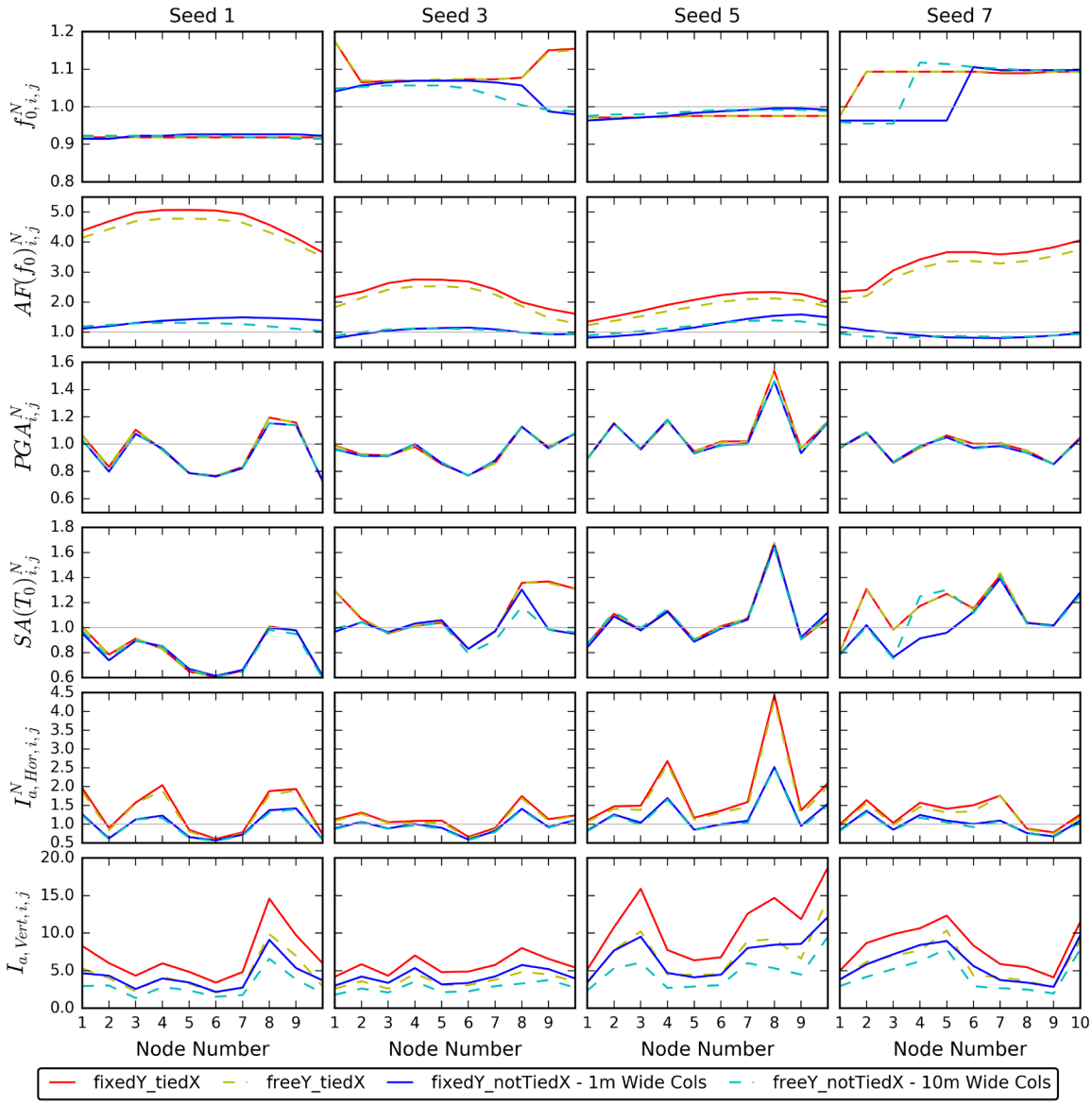

Figure 6: Normalised ground surface nodal IMs from four random field seeds comparing results from four variations of base conditions. Results are normalised by the equivalent $1D_{Det}$ value, except for $I_{a,Vert}$ which is zero for $1D_{Det}$.

3.3 Uniformity of horizontal displacements along base nodes

Another simplification is to tie all base nodes together so that their response is uniform, and the input motion need only be applied at one location (the master or retained node). By far, this is the most influential assumption analysed in this study. In order to release the base nodes so that they respond independently, each node must have its own horizontal dashpot. In the same manner as the vertical dashpots were created to make the base vertically compliant, a linear viscous material is applied to the zeroLengthElement connecting the dashpot nodes using a dashpot coefficient of $\rho V_S A_{trib}$. The input motion is then applied separately at each node as a dynamic force proportional to $\rho V_S A_{trib}$. Studies that have implemented model base conditions with individual horizontal dashpots on every base node to allow better base compliance include Zhang et al. (2003), Assimaki (2004), Elgamal et al. (2008), Zhang et al. 2008, Chavan and Prashant (2017), and Vytiniotis et al. (2019).

While the simplification that all base nodes move horizontally uniformly is appropriate for a homogeneous and level deposit, this assumption is not appropriate for 2D models with randomized properties or other

heterogeneities. The effect of this simplification is very visible in the frequency domain when comparing the amplification at f_0 in transfer functions between the 'tiedX' and 'notTiedX' cases. AF(f_0) is significantly larger for the model with a base tied horizontally (see Figs 4 and 5). This effect is also clearly visible in the time domain by directly comparing acceleration waveforms between the 'fixedY_tiedX' and 'freeY_notTiedX' cases in Figure 7. Higher horizontal accelerations occur in second arrivals (i.e., reflections off base) and subsequent coda when the base nodes are tied to each other, however the first arrival amplitudes are not affected. Similar behaviour is observed in a comparison of base and boundary conditions by Zhang et al. (2003). Waves that are reflected back down from the surface will arrive at the halfspace at different times due to the heterogeneities. This non-uniform wave field observes a base that behaves more as a rigid base because any force applied to the base must move the entire soil column (1,000 elements wide). This causes more energy to be reflected back into the model than is expected for a compliant base. Higher horizontal Arias intensity ($I_{a,Hor}$) for the 'tiedX' models, shown in Figure 6, confirms the increase in total energy trapped within the model. Peak intensity measures that are controlled by the first arrival (e.g., PGA and SA(T_0)) are not sensitive to the modifications of vertical and horizontal constraint analysed in this study (Fig. 6).

3.4 Width of massive free field columns

Initially, free field columns were only one-element-wide (i.e., 1-m-wide). This narrow column was insufficient to completely hold back soil pressures from the inner domain which caused bulging at the base of the columns and sagging of the base near the lateral extents. Widening the columns to encompass 10 elements significantly reduced the bulging and sagging that was observed. Figure 8 plots horizontal and vertical (X and Y, respectively) displacements along all base nodes for the 1-m- and 10-m-wide free field columns. Gravity and dynamic displacements are superimposed, and every tenth time step is plotted with time increasing on the colour scale from 0 (dark blue) to 30 s (dark red). These displacements show that the 1-m-wide columns were experiencing more horizontal displacements, indicating bulging, during the gravity analysis (time 0: dark blue), which continued to increase during the dynamic analysis. This bulging behaviour is not observed in 10-m-wide columns (right side of figure), however, some distortion along the base during the gravity analysis is unavoidable due to heterogeneities in soil stiffness which cause non-zero X-reactions in base nodes. The bulging and sagging of narrow columns was also influencing the response at low frequencies as observed in nodal transfer functions in the bottom left panel of Figure 4.

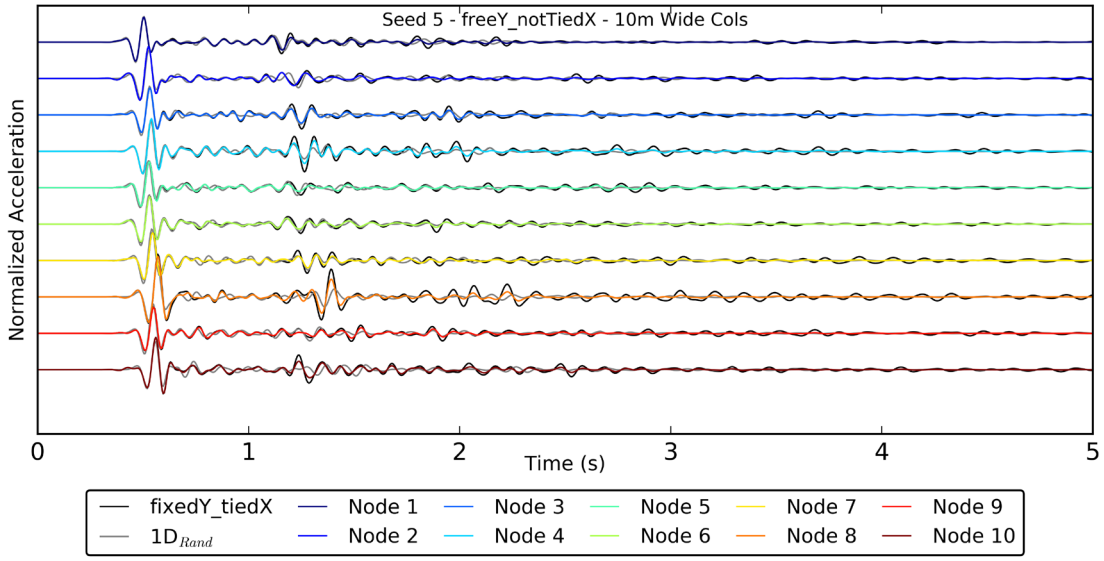

Figure 7: Comparison of normalised acceleration time series from one random field seed for the final proposed model configuration ('freeY_notTiedX'), and the original fixedY_tiedX model. Time series from 1D randomised ($1D_{Rand}$) profiles are also plotted for reference.

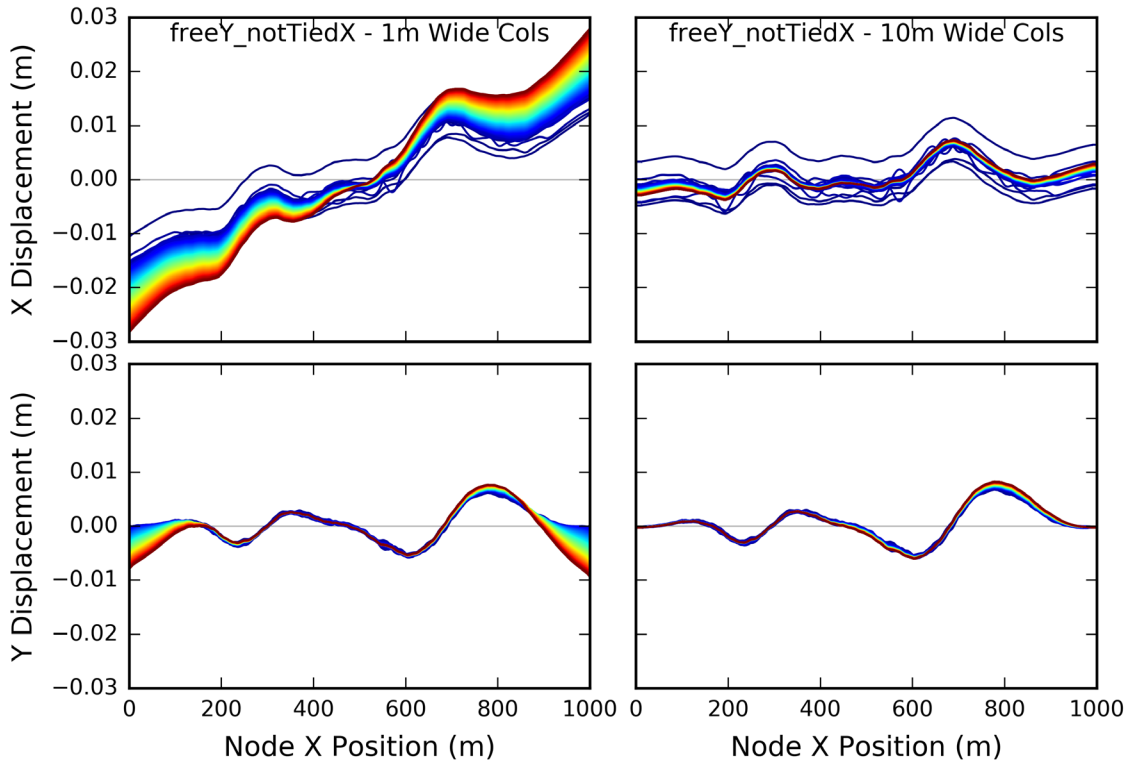

Figure 8: X and Y displacements as a function of X position for all nodes along the base of the model for the final proposed model configuration ('freeY_notTiedX'). Left and right panels are for 1-m-wide and 10-m-wide massive columns, respectively. Every tenth time step is plotted, with the color scale representing time increasing from dark blue at 0.0 seconds and to dark red at 30 seconds (end of record). Note that dynamic and 'static' gravity displacements are superimposed.

4 CONCLUSIONS

As part of the development of an approach for incorporating wave scattering and soil heterogeneity in conventional site response analysis by de la Torre et al. (2021), a detailed examination of various boundary conditions for 2D geotechnical earthquake analyses was conducted. The results and conclusions of this boundary condition assessment are presented in this current paper. Various modifications to the lateral and base boundaries were examined to assess their influence on the resulting surface ground motion. The final resulting model used for production analyses included massive 10-element-wide "free-field" columns on the lateral boundaries, and a base that is free in the vertical direction with nodes that are allowed to displace independently in both directions. It was found that in order to prevent spurious reflections from the base, a vertically and horizontally compliant base should be used, and each node along the base must be allowed to respond independently with its own dashpot (i.e., base nodes should not be tied to each other to respond in unison). Failure to implement such compliance and independence in the base nodes could result in overestimation of intensity measures (i.e., inefficient absorption of energy) because of the generation of vertical motion from refraction and wave scattering, and the lateral variation in arrival times of down-going waves at the base. 1-m-wide massive free columns were found to be too narrow to support the earth pressures from the interior model domain, therefore, columns were widened to 10 m (i.e., 10 elements wide). The use of massive "free-field" columns for lateral boundaries as opposed to periodic boundary conditions did not have a significant influence on results in the centre of the model.

5 REFERENCES

Assimaki, D., 2004. Topography Effects in the 1999 Athens Earthquake: Engineering Issues in Seismology. PhD thesis, Massachusetts Institute of Technology.

Assimaki, D., Pecker, A., Popescu, R., and Prevost, J., 2003. Effects of Spatial Variability of Soil Properties on Surface Ground Motion. *Journal of Earthquake Engineering* **7**, 1–44.

Chavan, D., G., M., and Prashant, A., 2017. Seismic analysis of nailed soil slope considering interface effects. *Soil Dynamics and Earthquake Engineering* **100**, 480–491.

Chin, C. Y., Kayser, C., and Pender, M., 2016. Seismic Earth Forces against Embedded Retaining Walls: Insights from Numerical Modelling. *Bulletin of the New Zealand Society for Earthquake Engineering* **49**.

de la Maza, G.,Williams, N., Saez, E., Rollins, K., and Ledezma, C., 2017. Liquefaction-Induced Lateral Spread in Lo Rojas, Coronel, Chile: Field Study and Numerical Modeling. *Earthquake Spectra* **33**, 219–240.

de la Torre, C., McGann, C. R., Bradley, B. A., and Pletzer, A., 2019. 3D Seismic Site Response with Soil Heterogeneity and Wave Scattering in OpenSees. In *The 1st Eurasian Conference on OpenSEES: OpenSEES Days Eurasia*, pp. 255–262.

de la Torre, C., Bradley, B. A., McGann, C. R., 2021. 2D Geotechnical Site-Response Analysis including Soil Heterogeneity and Wave Scattering. *Earthquake Spectra*. Under Review.

Elgamal, A., Yan, L., Yang, Z., and Conte, J., 2008. Three-Dimensional Seismic Response of Humboldt Bay Bridge-Foundation-Ground System. *Journal of Geotechnical and Geoenvironmental Engineering* **137**, 1165–1176.

Gobbi, S., Lopez-Caballero, F., and Forcellini, D., 2017. Numerical Analysis of Soil Liquefaction Induced Failure of Embankments. In *6th ECCOMAS Thematic Conference on Computational Methods in Structural Dynamics and Earthquake Engineering*.

Jeong, S. and Bradley, B., 2017. Amplification of Strong Ground Motions at Heathcote Valley during the 2010-2011 Canterbury Earthquakes: The Role of 2D Non-Linear Site Response. *Bulletin of the Seismological Society of America* **107**.

Karimi, Z. and Dashti, S., 2016. Numerical and Centrifuge Modeling of Seismic Soil–Foundation–Structure Interaction on Liquefiable Ground. *Journal of Geotechnical and Geoenvironmental Engineering* **142**, 04015061

McGann, C. and Arduino, P., 2015. Dynamic 2D Effective Stress Analysis of Slope. http://opensees.berkeley.edu/wiki/index.php/Dynamic_2D_Effective_Stress_Analysis_of_Slope.

McKenna, F., 2011. OpenSees: A framework for earthquake engineering simulation. *Computing in Science and Engineering* **13**, 58–66.

Ramirez, J., Barrero, A., Chen, L., Dashti., S., Ghofrani, A., Taiebat, M., and Arduino, P., 2018. Site Response in a Layered Liquefiable Deposit: Evaluation of Different Numerical Tools and Methodologies with Centrifuge Experimental Results. *Journal of Geotechnical and Geoenvironmental Engineering* **144**, 04018073.

Vytiniotis, A., Panagiotidou, A., and Whittle, A., 2019. Analysis of seismic damage mitigation for a pile-supported wharf structure. *Soil Dynamics and Earthquake Engineering* **119**, 21–35.

Zhang, Y., Conte, J., Yang, Z., Elgamal, A., Bielak, J., and Acero, G., 2008. Two-Dimensional Nonlinear Earthquake Response Analysis of a Bridge-Foundation-Ground System. *Earthquake Spectra* **24**, 343–386.

Zhang, Y., Yang, Z., Bielak, J., Conte, J., and Elgamal, A., 2003. Treatment of Seismic Input and Boundary Conditions in Nonlinear Seismic Analysis of a Bridge Ground System. In *16th ASCE Engineering Mechanics Conference*.